INSTITUTE OF PLASMA PHYSICS
CZECHOSLOVAK ACADEMY OF SCIENCES

ON OPTIMIZATION OF THE MULTIJUNCTION GRILL FOR THE LOWER HYBRID CURRENT DRIVE

J. Preinhaelter

RESEARCH REPORT

IPPCZ–280 April 1988

POD VODÁRENSKOU VĚŽÍ 4, 18069 PRAGUE 8
CZECHOSLOVAKIA

ON OPTIMIZATION OF THE MULTIJUNCTION GRILL FOR THE LOWER HYBRID CURRENT DRIVE

J. Preinhaelter

IPPCZ 280 April 1988

Abstract

Design of the multijunction grill which is supposed to be used in the current drive experiments calls for the optimization over three most important parameters: the phase shift $\Delta\phi$ among the adjacent waveguides, the length of the multijunction grill L_g (from the junction to the mouth) and the surface density n_0. This has been demonstrated on the results of the numerical investigation of the four-waveguide grill designed for a small tokamak. It has been shown that current drive efficiency (or the directivity) can reach 50 % for practically arbitrary $\Delta\phi$ ($\neq 0\,^\circ, 180\,^\circ$), if we choose L_g properly The enhanced current drive efficiency at $\Delta\phi \neq 90^\circ$ follows from an unevenly distributed power among the separate waveguides and from the selfadaptive adjustment of the phases of the incident waves. Risk of the power overloading of the waveguides grows with the decreasing n_0. A short description of the author's variant of the theory of the wave diffraction on the junction is given in Appendix.

1. Introduction

The waves having the frequency in the region of the lower hybrid resonance are now still more frequently used for the plasma heating and the non-inductive current drive. It is given both by the existence of the powerful sources of radiation working at several gigahertzs and by the possibility to control the profil of the current generated in this way and thus improve the plasma stability.

The slow-down structures known as the grills serve usually for the purpose of transmitting the power from a h.f. generator to a plasma. Originally, this structure was build from separate independently phased waveguides /1/. Later, it was proposed by D. Moreau and T. K. Nguyen to use a technically more simple structure: the multijunction grill /2/. In this concept the terminal part of the waveguide is split into several subsidiary waveguides by means of the dividers prependicular to the electric field of the incident TE_{10} mode. If we adjust the heights of the subsidiary waveguides properly, we obtain the necessary phase shift between waves radiated from the adjacent waveguides. At present time, three- or four-waveguide multijunction grills serve as construction elements of the large antena arrays for the large tokamaks /3/.

The original theory of the multijunction grill used the scattering matrix formalism and the complex power conservation law /4/. In our paper we are using the important statement from the general theory of the waveguide junctions: there are simple linear relations among the amplitudes of waves incident upon

and reflected from the junction /5/. The form of these relations is given in Sec. 2. In App. 1. we shortly describe how to obtain the numerical values of the coefficients in these relations. The method is based on the procedure applied by R. Mitra and S. W. Lee to the solution of the problem of the bifurcated waveguide /6/. By this way we obtain the amplitudes of waves incident upon a plasma from the subsidiary waveguides. If we insert these expressions into an arbitrary code of the conventional grill we can easily determine all needed quantities. We have used a code based on the standard Brambilla's theory /7/ with some extensions /8/, /9/.

Sec. 3. contains the numerical results which served for design of the four-waveguide multijunction grill mounted on the tokamak CASTOR /10/. Is is a small tokamak having a weak magnetic field ($B \sim 1.3\,T$) and bad energy confinement so that the spectrum required in the current drive experiment must be very broad ($1.5 < N_z < 10$, where $N_z = k_z / k_v$). The attention was concentrated on three main parameters which determine the grill efficiency: on the phase shift $\Delta\phi$ between the adjacent waveguides, on the length L_g of the multijunction grill[+)] and on the surface density n_0 of a plasma in front of the grill. A schematic view of this grill is given in Fig. 1.

+) The importance of this parameter at the multijunction grill design was pointed out by D. Moreau et al. in /16/ and systematically studied by autor in /11/.

The phase shifts and the reflection coefficients in the separate subsidiary waveguides are given in App. 2.

2. Summary of the theory of the multijunction grill

As it was stated in the Introduction, there are simple relations among the amplitudes of waves incident on and reflected from the junction. Thus we can write

$$A'_p = \alpha_{p0} A' + \sum_{j=1}^{N} \alpha_{pj} B'_j , \quad p = 1, 2, \ldots N \tag{1}$$

$$B' = \beta_0 A' + \sum_{j=1}^{N} \beta_j B'_j$$

where N is the number of the subsidiary waveguides in the multijunction grill, A'_p is the amplitude of wave propagating from the junction to the grill mouth in the p-th waveguide, B'_p corresponds to the wave reflected from a plasma to the junction in the same waveguide. A' and B' are the amplitudes of incident and reflected waves in the main waveguide, respectively. All these amplitudes correspond to TE_{10} modes and the particular expressions for the corresponding electric fields at the junction are given in App. 1.

The numerical value of the coefficients α_{pj} and β_j are determined from the continuity conditions of the tangential components of the electric and magnetic fields at the plane of the junction (see App. 1.).

When a wave passes the distance L_g between the junction and the grill mouth its phase increases by ϕ_p in the p-th waveguide. The phase ϕ_p can be expressed in a form

(2) $\phi_p = \phi_0 + (p-1)\,\Delta\phi\,, \quad p = 1, 2, \ldots, N.$

Travelling through the first waveguide (at $z = 0$) the wave acquires the phase ϕ_0 . If the first subsidiary waveguide has the same height a throughout, $\phi_0 = k_x L_g$ where $k_x = \left(k_w^2 - (\pi/a)^2\right)^{1/2}$

The intrinsic reflection in the subsidiary waveguides can be substantially diminished if we use $\lambda/4$ transformers to make smoother their height jumps /12/. Because the overall reflection coefficient of the multijunction grill is usually very small we investigate this problem more throughly in App. 2.

At the grill mouth, the z-component of the electric field of wave can be written

$$E_z = \sum_{p=1}^{N} \theta_p(z)\, e^{i(\phi_p - \omega t)} \Big\{ A_p e^{ik_v x} + B_p e^{-ik_v x} + \sum_{m=1}^{\infty} b_{pm}\, e^{\Gamma_{pm} x} \cos\left(\frac{m\pi}{b_p}(z - z_p)\right) \Big\} \tag{3}$$

Here, A_p and B_p are amplitudes of the incident and reflected waves at the grill mouth, respectively, z_p is the z-coordinate of the left wall of the p-th subsidiary waveguide ($z_1 = 0$), b_{pm} are the amplitudes of the evanescent modes, $\Gamma_{pm} = \left(m\pi/b_p\right)^2 - k_v^2\Big)^{1/2}$ $\theta_p(z) = 1$ in the p-th waveguide mouth and $\theta_p(z) = 0$ elsewhere. The parallel-plate waveguides ($a \to \infty$) are supposed.

For A_p and B_p we obtain

(4) $$A_p = \sqrt{\left(\frac{k_x}{2k_y}\right)}\, A'_p\,, \quad B_p = \sqrt{\left(\frac{k_x}{2k_y}\right)} e^{-2i\phi_p} B'_p$$

and thus

(5) $$A_p = \sqrt{\left(\frac{k_x}{2k_y}\right)} \alpha_{p0} A' + \sum_{j=1}^{N} e^{2i\phi_j} \alpha_{pj} B_j$$

The factor $(k_x/2k_y)^{1/2}$ ensures that the total energy flow through the section of the height a in the parallel-plate waveguide is equal to the total energy flow through the rectangular waveguide of the height a. It follows from (5), that the incident waves do not have the same amplitudes as it is usual in the conventional grill. Also their actual phases are not equal to ϕ_p because $\alpha_{p\,j}$ and B_p are generally complex. In the whole problem, the phase ϕ_o appears only in the equation (5) namely in the form $e^{2i\phi_o}$

Now we make use of the standard Brambilla's theory to solve the problem of the multijunction grill. The matching of fields in the grill mouth results in the following set of the equations for B_p and b_{pm} :

(6) $$\sum_{p=1}^{N} e^{i\phi_p}\left(B_q C^p_{ql} + \sum_{m=1}^{\alpha} b_{pm} C^{pm}_{ql}\right) = -\sum_{p=1}^{N} A_p e^{i\phi_p} P^p_{ql}\,, \quad q = 1,2,\ldots N, \quad l = 1,2\ldots$$

The explicit form of the coefficient C^p_{ql}, C^{pm}_{ql} and P^p_{ql} can be found e.g. in /8/. If we now insert A_p given (5) into

(6) we obtain the final set of the equations for the multi-junction grill:

$$\sum_{p=1}^{N} e^{i\phi_p} \left\{ B_p \left(C_{ql}^{p} + \sum_{r=1}^{N} e^{i(\phi_p + \phi_r)} \alpha_{rp} P_{ql}^{r} \right) + \right.$$

(7)

$$\left. + \sum_{m=1}^{\infty} b_{pm} C_{ql}^{pm} \right\} = -A' \sqrt{\left(\frac{k_x}{2k_r} \right)} \sum_{p=1}^{N} e^{i\phi_p} \alpha_{po} P_{ql}^{p}$$

Once this system is solved and B_p and b_{pm} are known, we can determine A_p and B' and thus we can easily compute the power spectrum and the reflection coeficients of the multi-junction grill.

3. Numerical results

As an example we present the results obtained at the optimization of the four-waveguide grill which was used in the lower hybrid current drive experiment on the small tokamak CASTOR /10/. The geometrical dimensions of this structure are following: the height of the main waveguide $a = 16\,cm$, its width $b = 4.6\,cm$, the width of the subsidiary waveguides $b_p = 1\,cm$ $(p = 1,2,3,4)$, the width of the dividers $d_p = 0.2\,cm$ and the length L_q of the structure is $95\,cm$, which is giving $\phi_0 = 45^\circ$ (see App. 2.). The working frequency is $1.25\,GHz$ and the phase shift $\Delta\phi$ between adjacent subsidiary waveguides is 120°. The plasma parameters in front of the grill we choose in accordonance with the measured values, viz. $n_e = 30\,n_{crit}$ ($n_{crit} = 2 \times 10^{10}\,cm^{-3}$) and $dn/dx = 8 \times 10^{11}\,cm^{-4}$

To describe the grill quality we shall use the following global quantities: the total power reflection coefficient R_t ($R_t \sim |B'|^2 b$), the total incident power in the grill mouth P_{in} ($P_{in} = \sum_{p=1}^{N} P_{in,p}$, where $P_{in,p} \sim |A_p|^2 b_p$ is the incident power in the p-th waveguide), the total reflected power in the grill mouth P_R ($P_R = \sum_{p=1}^{N} P_{R,p}$, where $P_{R,p} \sim |B_p|^2 b_p$) and the efficiency of the current generation η_{cur} given by

$$(8) \quad \eta_{cur} = (1 - R_t) \left\{ \int_0^\infty G(N_z) dN_z - \int_{-\infty}^{0} G(N_z) dN_z \right\},$$

where $G(N_z)$ is the normalized spectral density of the power radiated from the grill into the plasma ($\int_{-\infty}^{\infty} G(N_z) dN_z = 1$). The net power leaving the grill is then $1 - R_t$. It holds $1 - R_t = P_{in} - P_R$ All quantities are time averaged and R_t, P_{in}, P_R are normalized to the unit power of the h.f. generator. For the conventional grill we have $P_{in} = 1$ $P_{in,p} = 1/N$, $P_R = R_t$.

The quantity η_{cur} provides only a crude estimate of the actual current drive efficiency which can be lower or even higher than η_{cur} That is for two reasons: 1) the short wavelength part of the spectrum ($N_z \gg 1$) is usually absorbed in the scrape-off layer of the plasma and it does not contribute to the current; 2) the waves with N_z in the inaccessibility region ($1 < N_z < N_{z\,acc}$) are converted into the fast waves having weak damping and they also do not contribute to the current generation.

First, we shall pay attention to the effect of the phase shift $\Delta\phi$ on the functioning of our multijunction grill. Our results are collected in figs. 2 - 5 where we choose $\phi_0 = 45^\circ$ and the other parametersone can find at the beginning of the section.

As it is seen in fig. 2, R_t is very small for $\Delta\phi \in \epsilon (40^\circ, 140^\circ)$ but with the exception of $\Delta\phi \sim 135^\circ$ is at least 5 times greater than that given oy the approximate formula: $R_{t\,app} = \left((N-1)\, d_p\, 12 b_p\right)^2 \sim 0.004$ (see /12/). At the same time the average power density is 1.5 - 18 times greater than that in the conventional grill. Better insight into the power overloading of waveguides one can get from fig. 3, where the incident and reflected powers in the separate subsidiary waveguides are depicted as functions of $\Delta\phi$ The maximum electric field in the p-th waveguide can be estimated with the help of the quantity

$$(9) \qquad \varkappa_p = \left((P_{in,p})^{1/2} + (P_{r,p})^{1/2} \right) \left(b / b_p \right)^{1/2}$$

It determines how many times this field is larger than the incident electric field in the main waveguide (e.g. $\varkappa_g = 2.4$ at $\Delta\phi = \pi/4$). We can also see that in a broad interval of $\Delta\phi$ either third or fourth waveguides does not transmit any power. The phases of the incident and reflected waves are given in fig. 4. Abrupt changes of these phases coincide with $\Delta\phi$ where the corresponding power is zero or very small.

The redistribution of the incident power and the self-consistent set-up of phases are giving together the effect known as the selfadaptation. As a result of the selfadaption we have low R_t and an unusual dependence of η_{cur} on $\Delta\phi$. From fig. 2 we see that it has three maxima in which it reaches values about 50 %. For the conventional grill with the identical A_p in each waveguide and with constant phase shift, η_{cur} has only one maximum at $\Delta\phi = 90^\circ$. As we shall see later η_{cur} can reach value higher than 50 % at any $\Delta\phi \neq 0^\circ, 180^\circ$ if we choose ϕ_o properly. The enhanced current drive power of the multijunction grill can be understood if we notice that in favorable cases the amplitudes of the incident waves in the subsequent waveguides grow up. Same effect was observed by the author at the conventional grill with uneven amplitudes of the incident waves in the separate waveguides /13/.

The shapes of the power spectra are given in fig. 5 for some selected values of $\Delta\phi$ We can see that the maximum of $G(N_z)$ for $N_z > 0$ shifts again to larger N_z if $\Delta\phi$ grows up but this process is not so straightforward as for the conventional grill. E.g. the spectra for $\Delta\phi = 120^\circ$ and 135° coincide with one another for $N_z > 0$ but they have substantially different parasitic branches ($N_z < 0$). This gives much better conditions for the current drive at $\Delta\phi = 135^\circ$ than at $\Delta\phi = 120^\circ$.

The efficiency of the multijunction grill can be also influenced by varying its length L_g. The parameter L_g enters

in the theory only through ϕ_0. We have investigated the dependence of all quantities on ϕ_0 in three important cases of the phase shifts, viz. $\Delta\phi = 90°$, $\Delta\phi = 120°$ and $\Delta\phi = 180°$.

At $\Delta\phi = 90°$ the dependence of the global parameters on ϕ_0 is rather inexpressive. In this case η_{cur} has a flat maximum for $\phi_0 \in (135°, 180°)$ as it is seen in fig. 6. In the same interval $R_t \sim 2\,\%$ but the incident power is unevenly distributed among the subsidiary waveguides (see fig. 7). The phases of the incident waves are practically equal to ϕ_0 (see fig. 8). The spectra for different ϕ_0 differ one from another mainly in their parasitic branches (see fig. 9). Thus it seems that the multijunction grill with $\Delta\phi = 90°$ fits very well in the current drive experiments.

The case $\Delta\phi = 120°$ was fully discussed by the author in /11/ for the same grill. It follows from that analysis that the dependence of all quantities on ϕ_0 is more pronounced and thus the interval of the suitable ϕ_0 is narrower (in this case η_{cur} has a maximum at $\phi_0 = 70°$).

The last case which was investigated was that of $\Delta\phi = 180°$. Here, the spectra are symetrical with respect to $N_k = 0$ and thus $\eta_{cur} = 0$. The reflection coefficient R_t remains large for all ϕ_0 ($R_t \sim 26\,\%$ at $\phi_0 = 55°$ and $R_t \sim 21\,\%$ at $\phi_0 = 110°$). By varying ϕ_0 we can reach only redistribution of the incident power among the separate waveguides and slight modification of the spectra at $N_k \sim 1$

If $\phi_0 = 35^\circ$ the power is distributed evenly among the waveguides. At $\phi_0 = 160^\circ$ the radiation commes predominantly from the central waveguides ($P_{in,1} = 0.165$, $P_{in,2} = 0.394$) and the spectrum starts from $|N_z| > 5.6$. In turn at $\phi_0 = 90^\circ$ the outer waveguides transmit the great part of the power ($P_{in,1} = 0.36$, $P_{in,2} = 0.14$) and the spectrum contains a large proportion of waves with $N_z \sim 1$.

The parameters $\Delta\phi$ and ϕ_0 are fixed by the construction of the multijunction grill and cannot be changed during the operation. However, the magnitude of the surface density of a plasma has much deeper effect on the multijunction grill efficiency than it has on the efficiency of the conventional grill. The effect of the surface density on the reflection coefficient and the directivity was previously studied in /15/ and /16/. The surface density can be influenced by changing the plasma column position. Also non-linear effects can disturb the density in front of grill /14/.

From fig. 10 we can see, that the overloading of the grill is more severe at low densities. The reflection coefficient grows but not so sharply as in case of the conventional grill. The most interesting is behaviour of the current drive efficiency η_{cur}. It even can increase with lowering n_0 . As it is seen from fig. 11 the spectrum varies strongly with n_0 . At a low n_0 the multijunction grill radiates the h.f. power effectively due to selfadaptation but in the spectrum the waves with $N_z \sim 1$ are preferred. At the conventional grill the spectrum is kept fixed but R_t grows sharply if n_0 decreases.

4. Conclusions

Optimizing the multijunction grill for the lower hybrid current drive we would start with the choice of $\Delta\phi$ (the working frequency and the dimensions of waveguides are interlocked and usually fixed by other reasons). This gives us the requisite value of $\overline{N_z}$ where the spectrum has maximum. We need not now confine ourselves to $\Delta\phi = 90°$ which was only suitable for the conventional grill. Practically any arbitrary value of $\Delta\phi$ can give a sufficiently high value of η_{cur}. This can be attained by the choice of ϕ_0 (or the lenght L_g of the multijunction grill). At the same time the power is distributed unevenly among the subsidiary waveguides and the phases of the incident waves are not equal to designed ϕ_p. If it is possible the choice $\Delta\phi = 90°$ is practical because the current drive optimum can be reached in a broad interval of ϕ_0 One must also keep in mind that the lowering of the surface density can lead to the deterioration of the grill quality viz. in respect of the power overloading.

The theory of the wave diffraction on the junction is in App. 1 formulated in such a way that it can be used also for several junctions in a tandem and it respects fully all questions connected with the conditioned convergence /17/ of the problems where edges play role.

Acknowledgements

The author wishes to thank R. Klíma, L. Krlín, P. Pavlo and J. Ďatlov for valuable discussions.

Appendix 1. Determination of the coefficients α_{p0}, α_{pj} and β_j

In the vicinity of the junction the z-component of the electric field of the wave in the main waveguide ($x < -L_g$) can be written as

$$E_z = \sin\frac{\pi y}{a}\left\{A' e^{ik_x(x+L_g)} + B' e^{-ik_x(x+L_g)} + \sum_{n=1}^{\infty} a_n \cos\left(\frac{n\pi}{b} z\right) e^{\gamma_n (x+L_g)}\right\}. \tag{10}$$

Here $\gamma_n \left((n\pi/b)^2 + (\pi/a)^2 - k_v^2\right)^{1/2}$ and a_n are the amplitudes of the evenescent modes. The expressions for E_x, H_x, H_y, H_z can be easily obtained and $E_y = 0$.

The fields in the subsidiary waveguides have similar shapes and e.g. again for E_z we have

$$E_z = \sin\frac{\pi y}{a}\left\{A'_p e^{ik_x(x+L_g)} + B'_p e^{-ik_x(x+L_g)} + \sum_{n=1}^{\infty} a_{pn} \cos\left(\frac{n\pi}{b_p}(z - z_p)\right) e^{-\gamma_{pn}(x+L_g)}\right\} \tag{11}$$

Here $\gamma_{pn} = \left((n\pi/b_p)^2 + (\pi/a)^2 - k_v^2\right)^{1/2}$ and a_{pn} are the amplitudes of the evanescent modes. The expression (11) is valid for $x > -L_g$ and $z \in (z_p, z_p + b_p)$.

Before matching fields at $x = -L_g$ it is suitable to suppose for some moment that the faces at the dividers are shifted to $x = -L_g + \delta$. Then we can express E_z and H_y as the fields in shallow short-circuited waveguides which had arisen in this way (see /6/).

The conditions of the continuity of E_z and H_y (H_x is then continuous automatically) in the z-representation are not apt for the numerical solution. Thus we carry out their Fourier analysis. If we perform the limit $\delta \to 0$ and eliminate a_{pn} we obtain the final set of the linear equations for a_n and B'. From the continuity of E_z and H_y in the mouths of the subsidiary waveguides we have

$$B' + \frac{1}{2} \sum_{n=1}^{\infty} R(p,n)\left(1 - i\frac{k_x}{\gamma_n}\right) a_n = B'_p, \tag{12}$$

$$\sum_{n=1}^{\infty} R(p,l,n)\left(\frac{k_y}{\gamma_n} + \frac{k_y}{\gamma_{pl}}\right) a_n = 0, \quad \begin{matrix} p = 1,2,\dots,N \\ l = 1,2,3,\dots \end{matrix} \tag{13}$$

The condition of $E_z = 0$ on the faces of the dividers gives

$$B' + \sum_{n=1}^{\infty} \bar{R}(p,n)\, a_n = -A', \qquad p = 1,2,\dots N-1 \tag{14}$$

$$\sum_{n=1}^{\infty} \bar{R}(p,l,n)\, a_n = 0, \qquad l = 1,2,3,\dots \tag{15}$$

Here

$$R(p,n) = \frac{1}{b_p} \int_{z_p}^{z_p + b_p} \cos\left(\frac{n\pi}{b} z\right) dz,$$

$$R(p,l,n) = \int_{z_p}^{z_p + b_p} \cos\left(\frac{n\pi}{b} z\right) \cos\left(\frac{l\pi(z - z_p)}{b_p}\right) dz,$$

$$\bar{R}(p,n) = \frac{1}{d_p} \int_{z_p + b_p}^{z_{p+1}} \cos\left(\frac{n\pi}{b} z\right) dz,$$

$$\bar{R}(p,l,n)=\int_{z_p+b_p}^{z_{p+1}}\cos\left(\frac{n\pi}{t}z\right)\cos\left(\frac{l\pi}{d_i}\left(z-z_p-b_p\right)\right)dz$$

We also get the equations for

(16) $$A'_p=A'+\frac{1}{2}\sum_{n=1}^{\infty}a_n R(p,n)\left(1+\frac{ik_x}{\gamma_n}\right),\quad p=1,2,\ldots,N.$$

To obtain the general solution of the set (12) - (15) we must solve these equations for the following $(N+1)$ choices of the right-hand sides:

$$A'=0,\quad B'_1=1,\quad B'_2=0,\ \ldots\ldots\ldots,B'_N=0$$

$$A'=0,\quad B'_1=0,\quad B'_2=1,\ B_3=0,\ldots\ldots,B'_N=0$$

$$A'=0,\quad B'_1=0,\ldots\ldots\ldots\ldots\ldots B'_{N-1}=0,\ B'_N=1,$$

$$A'=1,\quad B'_1=0,\ldots\ldots\ldots\ldots\ldots\ldots\ B'_N=0$$

In this way we acquire $(N+1)$ solutions $B'^{(j)}, a_1^{(j)}, a_2^{(j)}\ldots$ where $j=1,2,\ldots N,N+1$. The general solution of the set has then a form

(17) $$B'=\sum_{j=1}^{N}B'^{(j)}B'_j+B'^{(N+1)}A'$$

$$a_k=\sum_{j=1}^{N}a_k^{(j)}B'_j+a_k^{(N+1)}A'$$

If we compere (17) with (1) we have $\beta_0 = B'^{(N+1)}$ and $\beta_j = B'^{(j)}$ where $j = 1, 2, \ldots N$. If we insert a_l given by (17) into (16) and compare with (1) we obtain

$$\alpha_{p0} = 1 + \frac{1}{2} \sum_{n=1}^{\infty} a_n^{(N+1)} R(p,n) \left(1 + \frac{ik_x}{\gamma_n} \right)$$

(18)

$$\alpha_{pj} = \frac{1}{2} \sum_{n=1}^{\infty} a_n^{(j)} R(p,n) \left(1 + \frac{ik_x}{\gamma_n} \right), \quad p,j = 1,2,\ldots,N.$$

Now we make a short comment to the numerical procedure used for the solution of the set (12) - (15). This infinite set corresponds to the problem of the diffraction of waves on an object with edges. Such a set has an infinite number of the solutions and only one has physical meaning (see /5 - 6/). To obtain this correct solution numerically we must choose the numbers of modes in the separate waveguides in proper way. We proceed in similar way as R. Mitra when he solved the diffraction of waves in the bifurcated parallel-plate waveguide /6/. Thus we pick up the number of modes in the separate waveguides proportional to their width. For our grill $b : b_p : d_p : 25 : 5 : 1$. The total number of modes to the right of the junction must be same as the number to the left of the junction. Thus, if we take 46 modes in the main waveguides, we have 10 modes in each subsidiary waveguide and 2 modes on each divider face. With this choice of mode numbers the sequence of a_n converges well and the energy flow across the junction is conserved to eight digits.

Appendix 2. The phase shifts and the reflection coefficients in the subsidiary waveguides

The section through one from the subsidiary waveguides is given in fig. 12. Here a_i are the heights of the separate section of the waveguide and $a_1 = a_5 = a$ and also $a_2 = a_4$. We suppose that only TE_{10} modes can propagate in each section so that $\lambda_v/2 < a < \lambda_v$ where $\lambda_v = 2\pi/k_v$. It is clear that the minimum wave reflection sets in if $L_2 - L_1 = L_4 - L_3 = \frac{\lambda_2}{4}$ ($\lambda/4$ transformers) and if also $L_3 - L_2 = l\lambda_3/2$, where l is an integer, $\lambda_i = 2\pi/k_{xi}$ and $k_{xi} = \left(k_v^2 - (\pi/a_i)^2\right)^{1/2}$. The last condition cannot be fulfilled exactly in all waveguides because we would not be able to reach the required phase shifts between the adjacent waveguides.

The multijunction grill have usually a very small reflection coefficient and thus it is important to have a very small intrinsic wave reflection in the subsidiary waveguides (we set it to zero so far). Also we must verify if the steps in the waveguide height have some other effect on the wave phase then that given by summing the terms $k_{xi}(L_{i+1} - L_i)$.

For these reasons we made a control numerical solution of the wave diffraction on the structure from fig. 12. The electric field at the i-th step ($x' < -L_i$) is composed from $TE_{3n,0}$ modes only and its z-component has form

$$E_z = \sin\frac{\pi(2y'+a_i)}{2a_i}\left\{A'_i e^{ik_{xi}x'} + B'_i e^{-ik_{xi}x'}\right\}$$

$$+\sum_{n=1}^{\infty} a_{ni}\sin\frac{(2n+1)\pi(2y'+a_i)}{2a_i}\, e^{\gamma_{2n+1,i}(x'-L_i)} \qquad (19)$$

where $x' = x + L_5$, $y' = y - a_1/2$ and $\gamma_{ni} = \left((n\pi/a_i)^2 - k_y^2\right)^{1/2}$. The evanescent modes can be considered locally only when the discontinuities are well separated (i.e. $\exp(-(3\pi/a_i)(L_{i+1}-L_i)) \ll 1$). On the other side of the discontinuity ($x' > L_i$) an expression similar to (19) can be written for the field.

By matching E_z and H_y in the mouth of the narrower waveguide and setting $E_z = 0$ on the step faces (see /6/) we obtain a set of the equations for a_{ni}. From the general solution of this system we get the relations connecting A'_i and B'_i with A'_{i+1} and B'_{i+1}. Using these relations for $i = 1,2,3,4$ we obtain finally the relations among the amplitudes A'_1 and B'_1 at $x' = 0$ and the amplitudes A'_5 and B'_5 at $x' = L_5$:

$$A'_5 = Q A'_1 + R B'_1$$
$$B'_5 = R^* A'_1 + Q^* B'_1 \qquad (20)$$

Fig. 13 shows the dependence of $|R|$ and $\phi = \arg(Q)$ on $L_1 - L_2 = L_4 - L_3$ ($L_3 - L_2$ is kept fixed) for the separate waveguides of the four-waveguide multijunction grill for CASTOR. Here $a_1 = a_5 = 16\,cm$, $L_2 = 20\,cm$, $L_3 = 70\,cm$ and $L_5 = L_8 = 95\,cm$. The amplitudes of the reflected waves in the first and the third waveguides are 10^{-3} – times smaller than these of the incident waves. In the second waveguide it is only 10^{-2} – times because $L_3 - L_2 \sim 5\lambda_2/4$. The fourth waveguide is identical with the first. The reflection minima are approximately at

$L_2 - L_1 \approx \lambda_2 / 4$ and the phase coincides (to $1°$) with the phase computed from the propagation of TE_{10} mode only.

References

/1/ P. Lallia, in Proc. 2nd Top. Conf. on R.F. Plasma Heating, Lubbock (1974), C3.

/2/ T. K. Nguyen and D. Moreau, in "Fusion Technology 1982", (Proc. 12th Symp. Jülich), Vol. 2 (1982) 1381.

/3/ G. Briffod and T. K. Nguyen, Un nouveau type de coupleur pour la generation de courant et le chauffage par les ondes hybrides sur les grands tokamaks, Fontenay-aux--Roses, Rep. EUR-CEA-FC-1326 (1987).

/4/ D. Moreau and T. K. Nguyen, Couplage de l'onde lente au voisinage de la fréguence hybride basse dans les grands tokamaks, Association Euratom-CEA, Centre d'études nucléaires de Fontenay-aux-Roses, Rep. EUR-CEA-FC-1246 (1983-84).

/5/ D. S. Jones, The theory of electromagnetism (Pergamon Press, Oxford, 1964).

/6/ R. Mitre and S. W. Lee, Analytical techniques in the theory of guided waves (The Macmillen Company, New York, 1971).

/7/ M. Brambilla, Nucl. Fusion, Vol. 16 (1976) 47.

/8/ Yu. F. Baranov, O. N. Shcherbinin, Fiz. Plazmy 3 (1977) 246.

/9/ J. Stevens, M. Cno, R. Horton, J. R. Wilson, Nucl. Fus. 21 (1981) 1259.

/10/ F. Žáček, J. Badalec, J. Ďatlov, K. Jakubka, V. Kopecký, et al., in Proc. of IAEA Technical Committee Meeting on Research using small tokamaks, Nagoya (1986) (in press), see also Rep. IPPCZ-273, Prague (1987).

/11/ J. Preinhaelter, Rep. IPPCZ-283, Prague (1988).

/12/ C. Gormezano, P. Briand, G. Briffod, G. T. Hoang, T. K. N'guyen, et al., Nucl. Fus. 25 (1985) 419.

/13/ J. Preinhaelter, in Radiation in Plasmas, Proc. 1983 College on Plasma Physics, Trieste, ed by B. McNamara, Vol. II, p. 813, World Scientific, Singapore, 1984.

/14/ V. Petržílka, R. Klíma, P. Pavlo, Czech. J. Phys. B33 (1983) 1002.

/15/ D. Moreau and T. K. Nguyen, in Proc. 1984 Int. Conf. on Plasma Physics, Lausanne, Vol. 1., (1984) 216.

/16/ D. Moreau, C. David, C. Gormezano, S. Knowlton, R. J. Anderson, et al., in Proc. of 7th AIP Conf. on Applic. of R. F. Power to Plasmas, Kissimmee (1987).

/17/ C. P. Wu, in Computer techniques for electromagnetics, ed. by R. Mitra, Pergamon Press, Oxford (1973).

Figure captions

Fig. 1 Schematic sketch of the multijunction grill facing a plasma with the step and ramp profile. (The auxiliary quantities $Z = -i \times 10^{-3}$ and $x_p = 0.01/k_v$ in numerical computations.)

Fig. 2 Dependence of the global parameters determining the grill efficiency on $\Delta\phi$. The phase $\phi_0 = 45^\circ$, the other parameters of the four-waveguide grill and plasma are given at the beginning of Sec. 3.

Fig. 3 Incident and reflected powers in the separate subsidiary waveguides as functions of $\Delta\phi$. For the other parameters see Fig. 2.

Fig. 4 Phases of the incident ($\phi_{in,p}$) and reflected ($\phi_{n,p}$) waves in the separate waveguides as functions of $\Delta\phi$. For the other parameters see Fig. 2.

Fig. 5 Power spectra of waves radiated from the grill into a plasma for different values of $\Delta\phi$ ($\Delta\phi = 90^\circ$ full line, $\Delta\phi = 120^\circ$ - dotted line, $\Delta\phi = 135^\circ$ - dashed line, $\Delta\phi = 180^\circ$ - dotted-and-dashed line). For the other parameters see Fig. 2.

Fig. 6 Dependence of the global parameters determining the grill efficiency on ϕ_0. The phase shift $\Delta\phi = 90^\circ$ The other parameters are given in the beginning of Sec. 3.

Fig. 7 Incident and reflected powers in the separate subsidiary waveguides as functions of ϕ_0. For the other para-

meters see Fig. 6.

Fig. 8 Phases of the incident and reflected waves in the separate waveguides as functions of ϕ_0 . For the other parameters see Fig. 6.

Fig. 9 Power spectra of waves radiated from the grill into a plasma for different values of ϕ_0 ($\phi_0 = 0°$ – full line, $\phi_0 = 90°$ - dashed line, $\phi_0 = 126°$ – dotted line).

Fig. 10 Dependence of the global parameters determining the grill efficiency on the density in front of the grill mouth. The phase shift $\Delta\phi = 120°$, the full line corresponds to $\phi_0 = 45°$ and the dashed line to $\phi_0 = 72°$; the other parameters are given at the beginning of Sec. 3.

Fig. 11 Power spectra of waves radiated from the grill into a plasma for different values of n_0 ($n_0 = 0$ – full line, $n_0 = 20\, n_{crit}$ - dashed line). The phase shift $\Delta\phi = 120°$ and $\phi_0 = 72°$.

Fig. 12 Section through one from the subsidiary waveguides.

Fig. 13 Amplitude of the reflection coefficient $|R|$ and the phase change ϕ_p of wave in the separate subsidiary waveguides as functions of $L_2 - L_1$; a) in the first waveguide $a_2 = 14.7\,cm$, $a_3 = 13.5\,cm$; b) in the second waveguide $a_2 = 15.5\,cm$, $a_3 = 15\,cm$; c) in the third waveguide $a_2 = 17\,cm$, $a_3 = 17.9\,cm$.

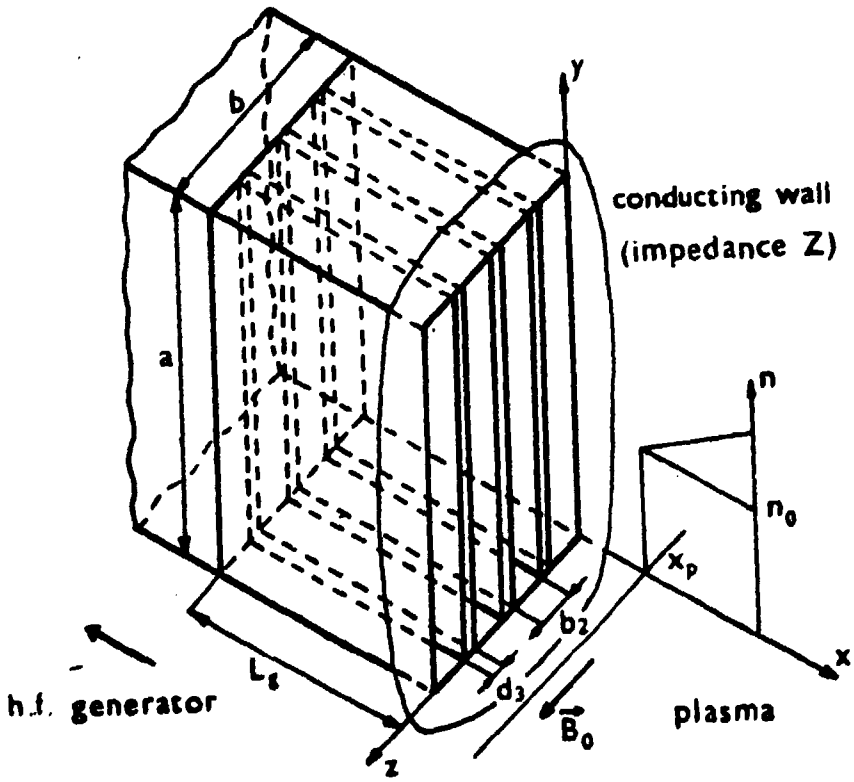
b
a
y
conducting wall
(impedance Z)
n
n_0
x_p
x
b_2
d_3
L_s
h.f. generator
$\vec{B}_0$
plasma
z

Fig. 1

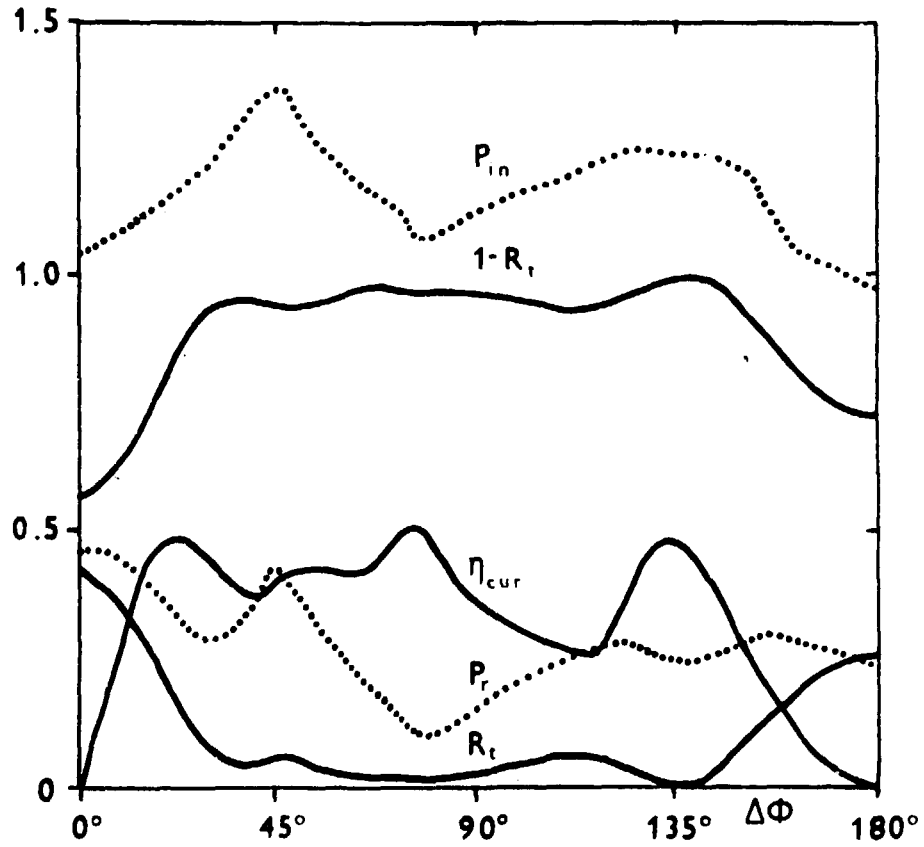

Fig. 2

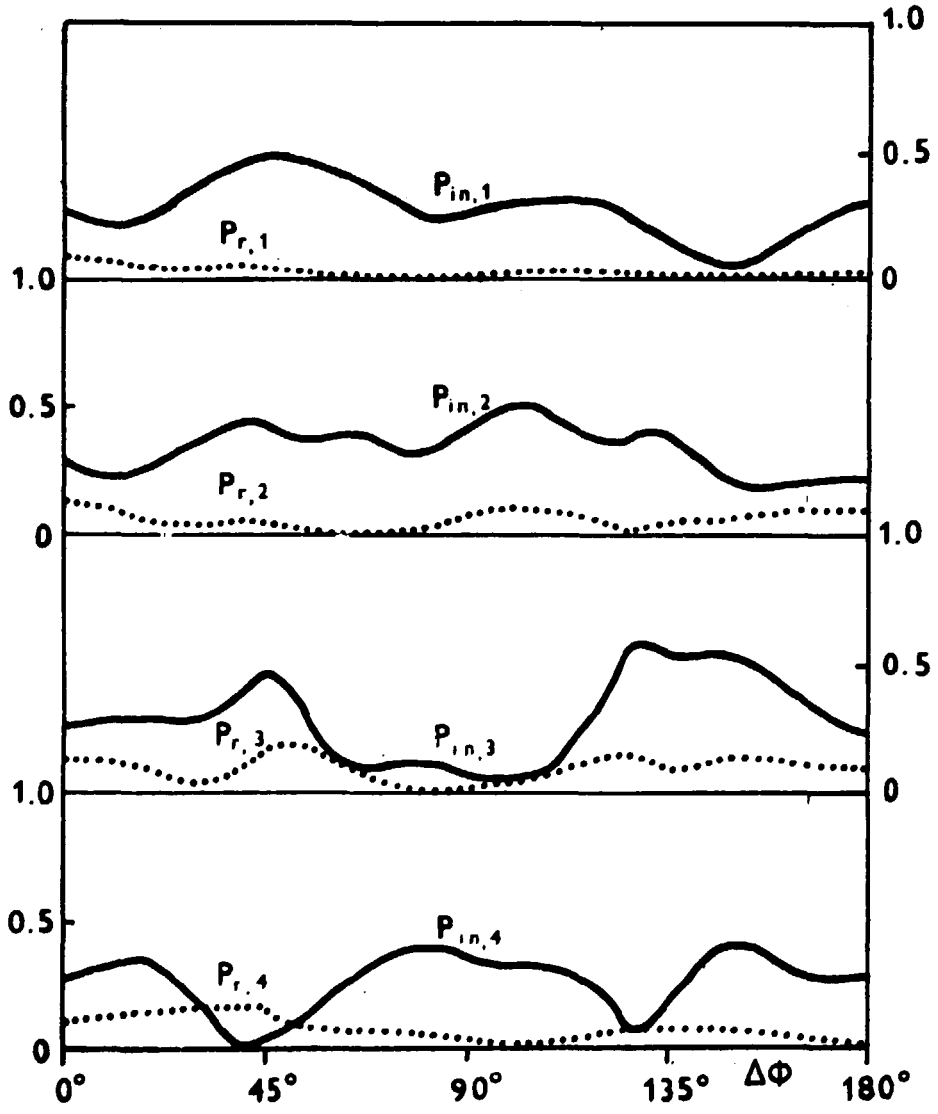
1.0
0.5
0
$P_{in,1}$
$P_{r,1}$
1.0
0.5
0
$P_{in,2}$
$P_{r,2}$
1.0
0.5
0
$P_{r,3}$
$P_{in,3}$
1.0
0.5
0
$P_{in,4}$
$P_{r,4}$
0°
45°
90°
135°
ΔΦ
180°

Fig. 3

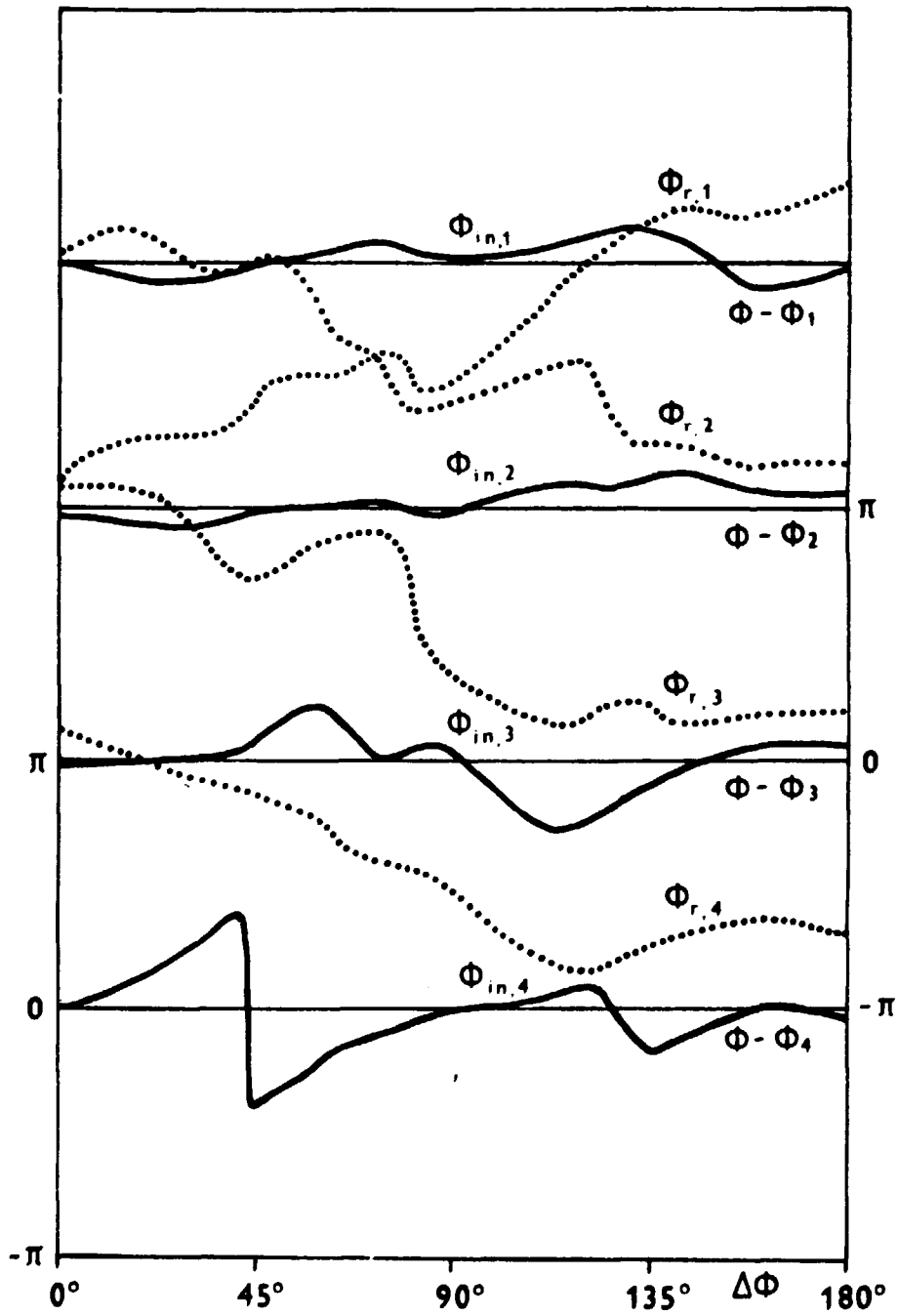
Φr,1
Φin,1
Φ - Φ1
Φr,2
Φin,2
π
Φ - Φ2
Φr,3
Φin,3
π
0
Φ - Φ3
Φr,4
Φin,4
0
-π
Φ - Φ4
-π
0°
45°
90°
135°
ΔΦ
180°

Fig. 4

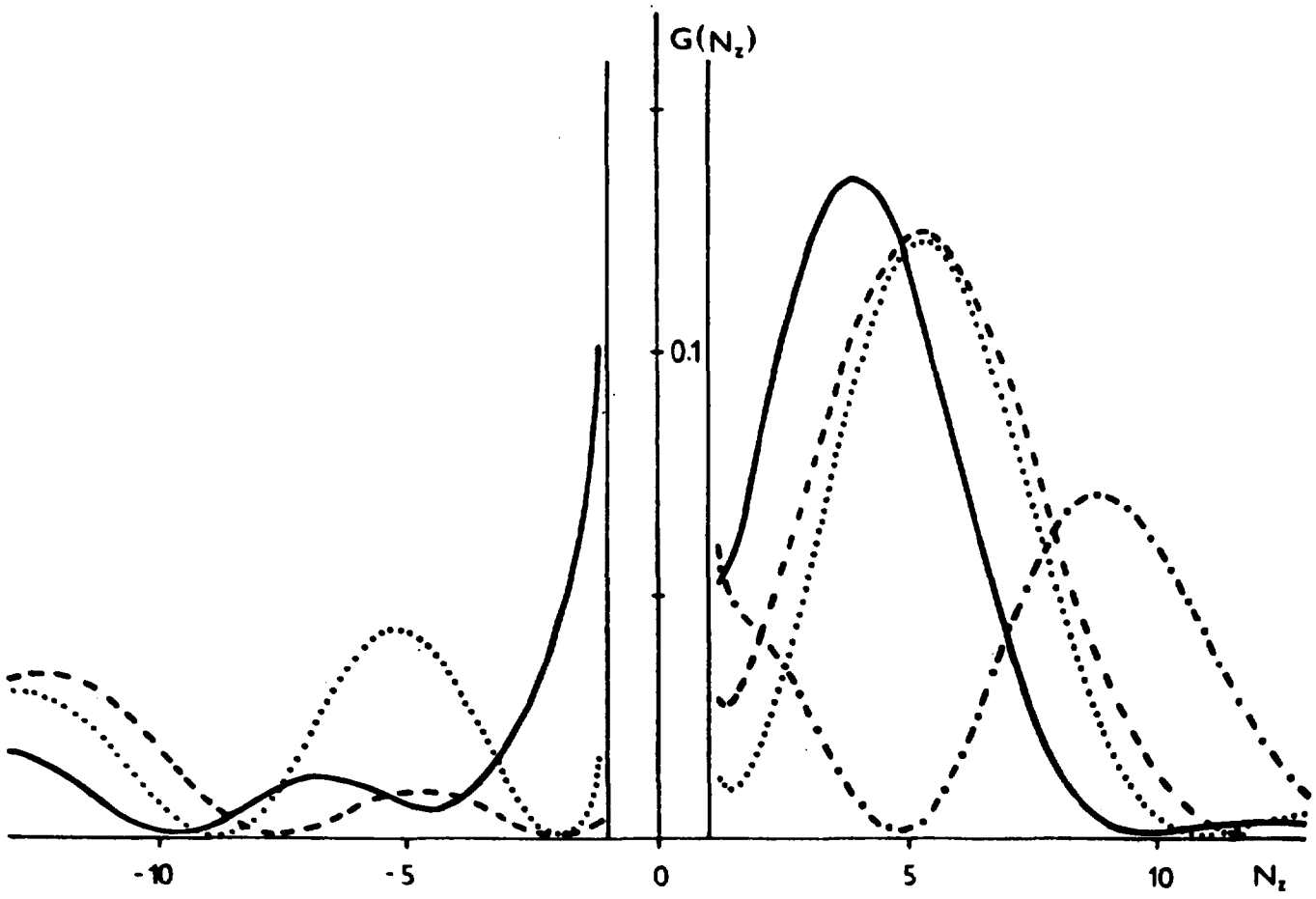

Fig. 5

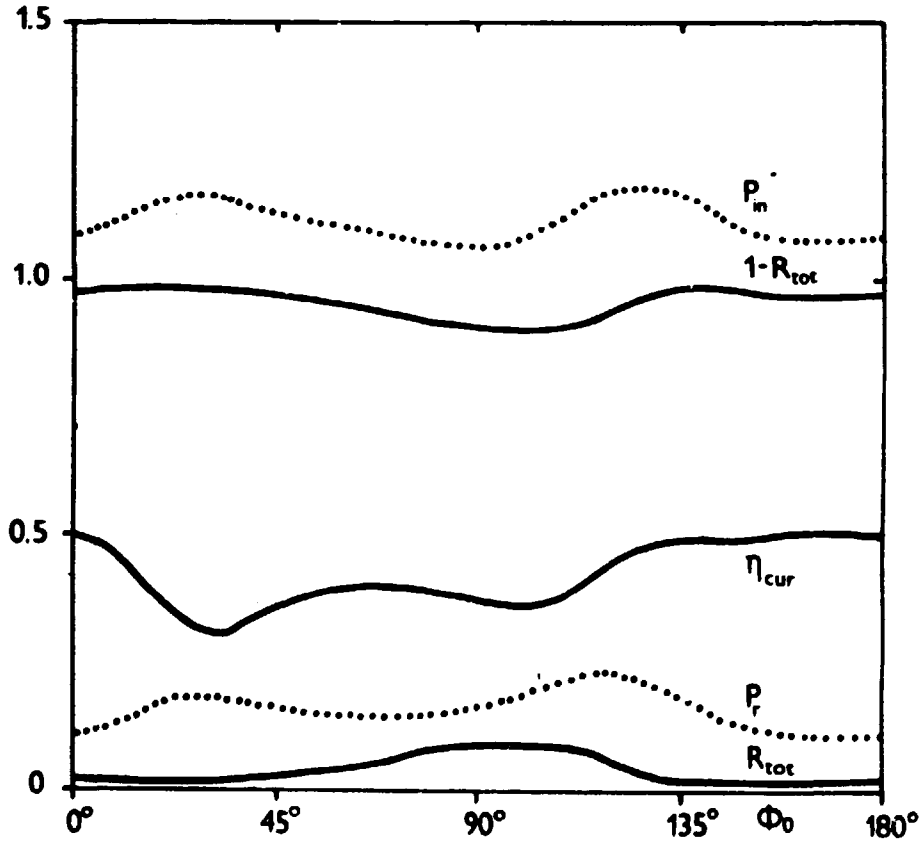

Fig. 6

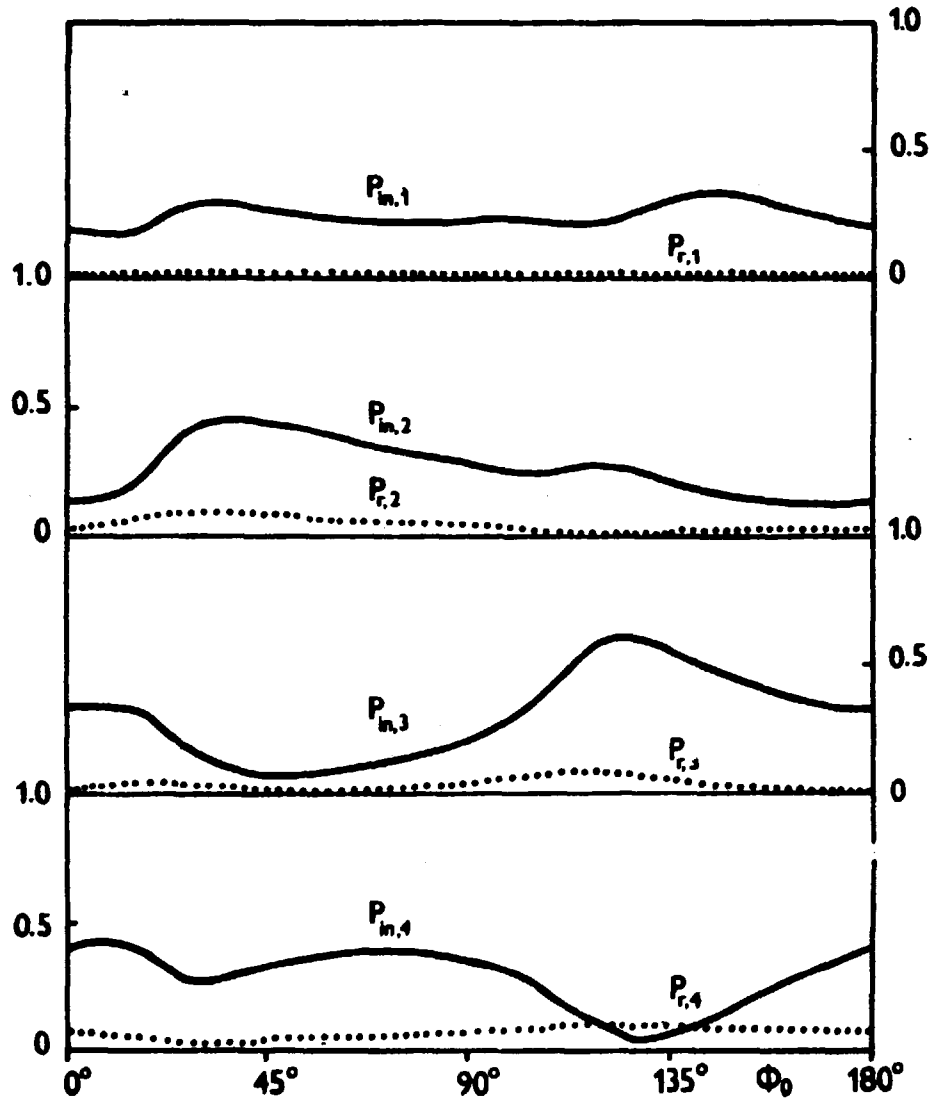
1.0
0.5
0
$P_{in,1}$
$P_{r,1}$
1.0
0.5
0
$P_{in,2}$
$P_{r,2}$
1.0
0.5
0
$P_{in,3}$
$P_{r,3}$
1.0
0.5
0
$P_{in,4}$
$P_{r,4}$
0°
45°
90°
135°
Φ_0
180°

Fig. 7

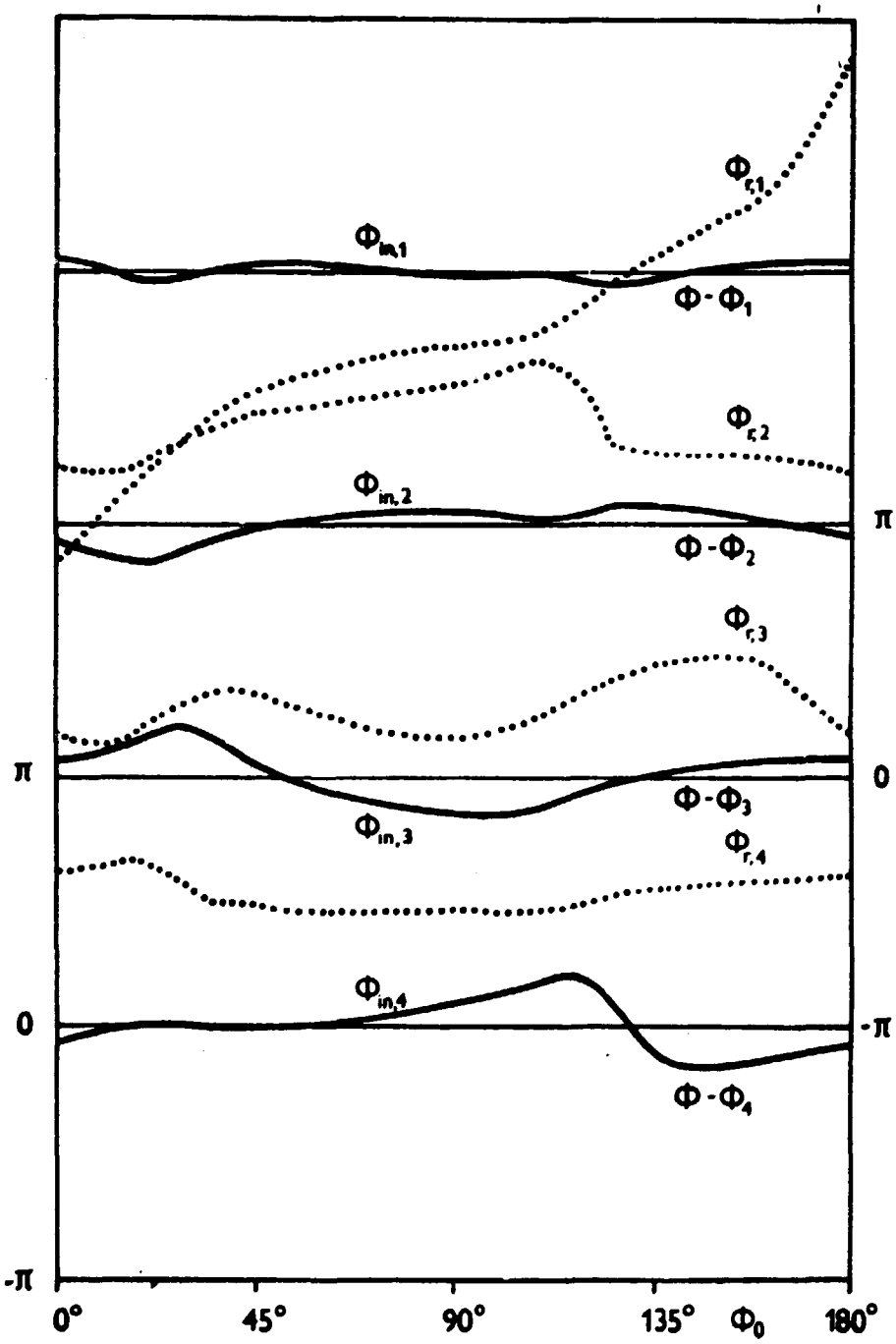
$\Phi_{r,1}$
$\Phi_{in,1}$
$\Phi - \Phi_1$
$\Phi_{r,2}$
$\Phi_{in,2}$
$\Phi - \Phi_2$
$\Phi_{r,3}$
$\Phi - \Phi_3$
$\Phi_{in,3}$
$\Phi_{r,4}$
$\Phi_{in,4}$
$\Phi - \Phi_4$
π
0
-π
0°
45°
90°
135°
Φ_0
180°

Fig. 8

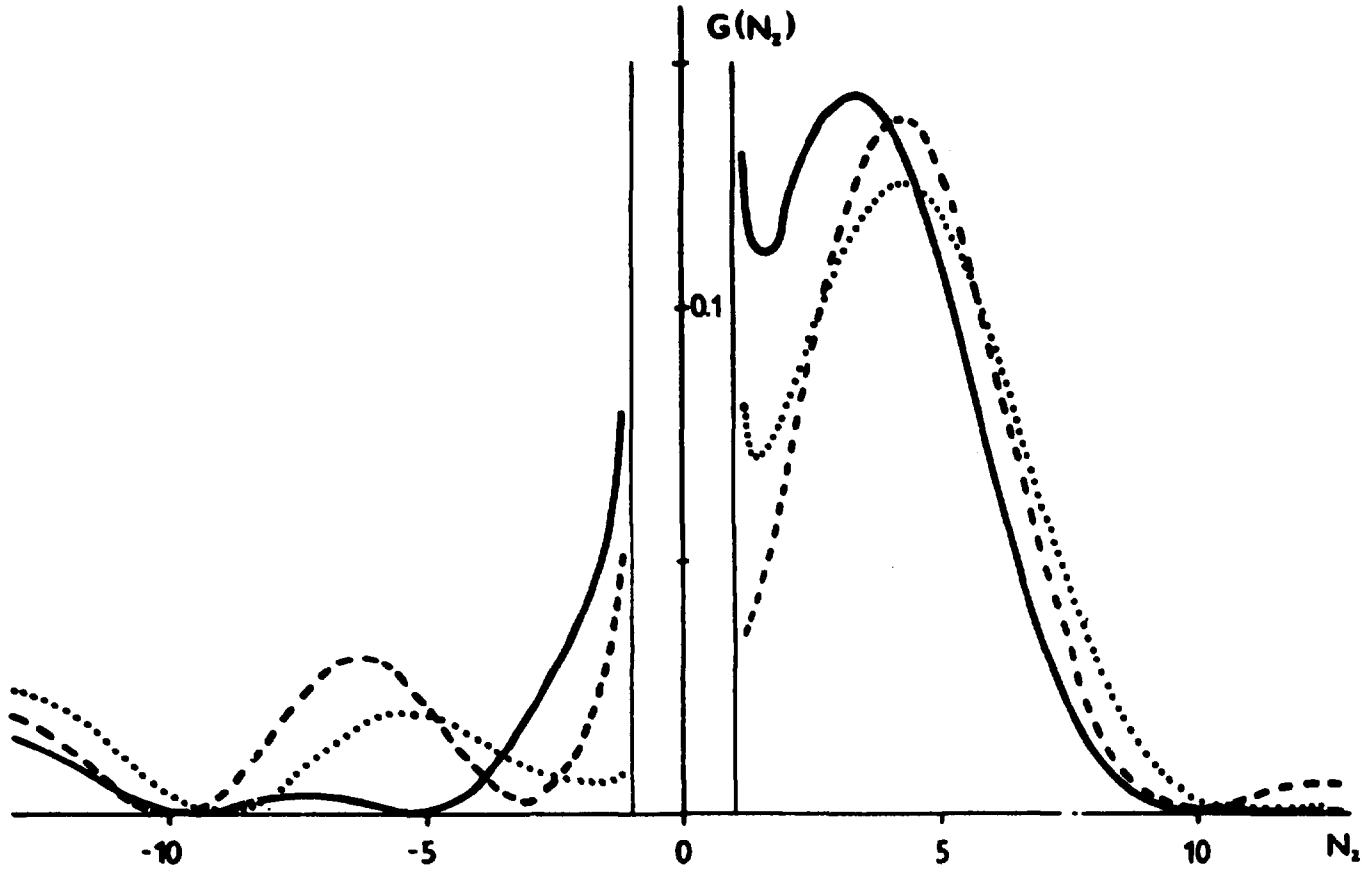

Fig. 9

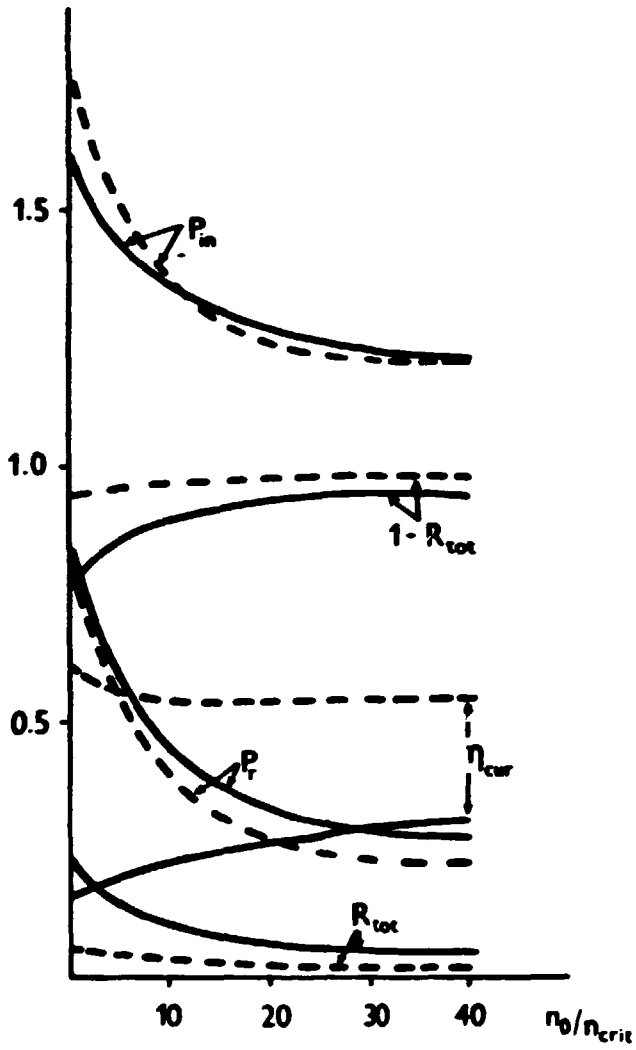
1.5
1.0
0.5
P_{in}
$1-R_{tot}$
P_r
η_{cur}
R_{tot}
10
20
30
40
n_0/n_{crit}

Fig. 10

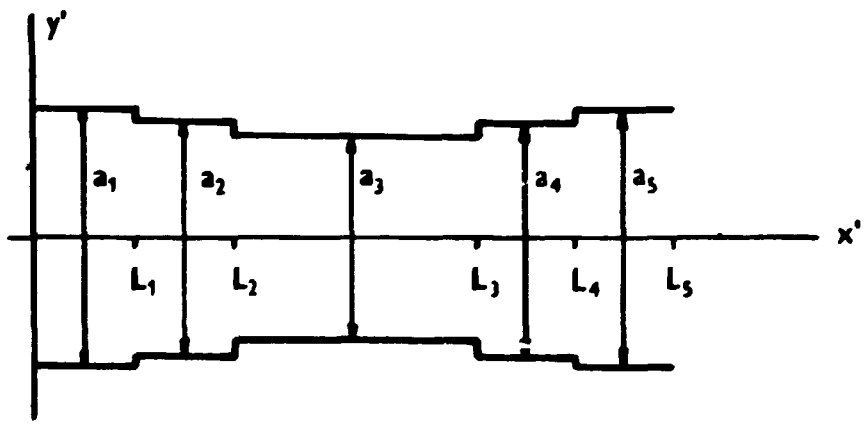
y'
x'
a_1
a_2
a_3
a_4
a_5
L_1
L_2
L_3
L_4
L_5

Fig. 12

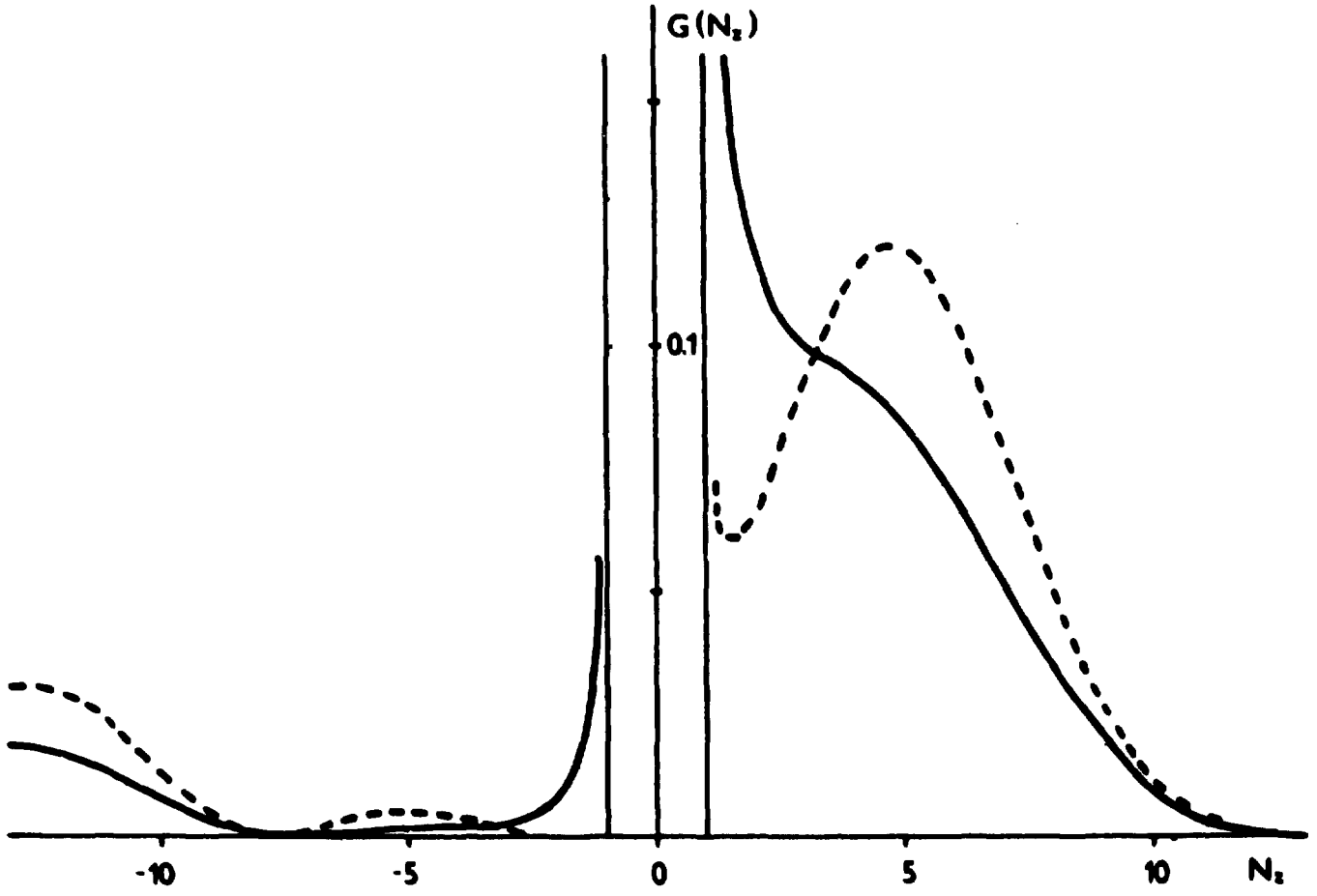

Fig. 11

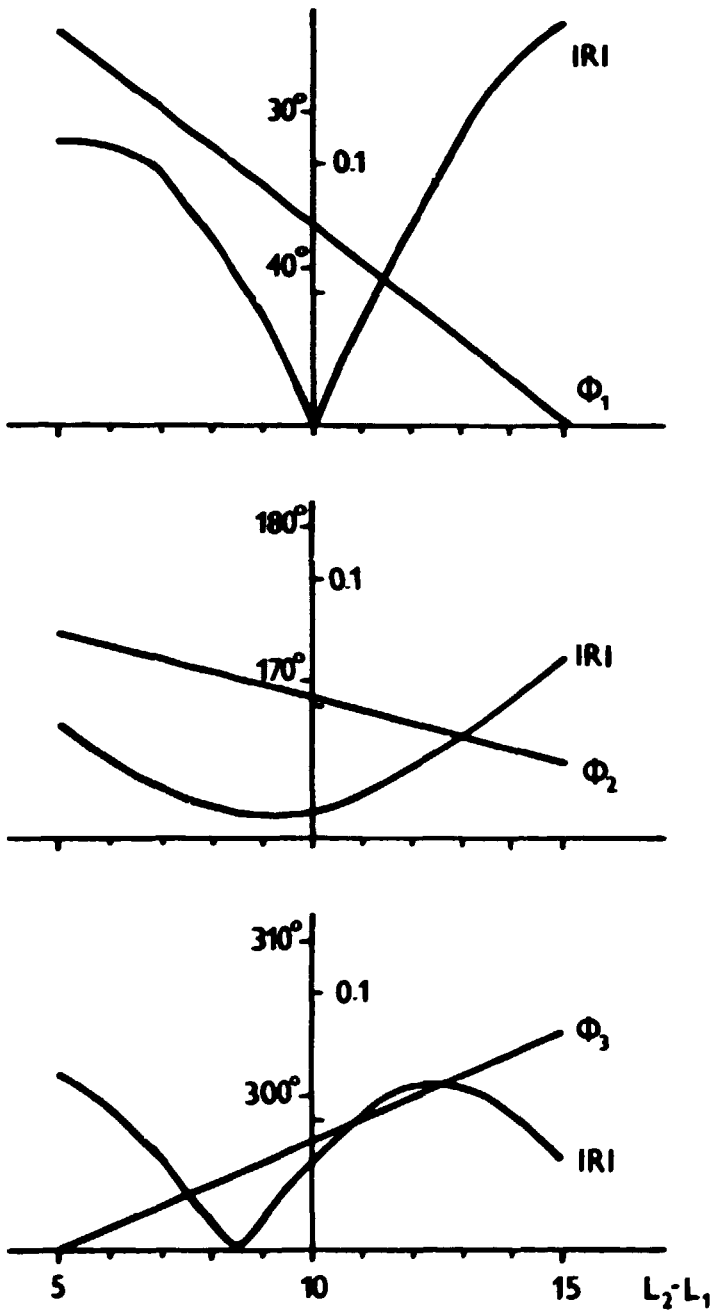

Fig. 13

TZ 56